Accepted Manuscript

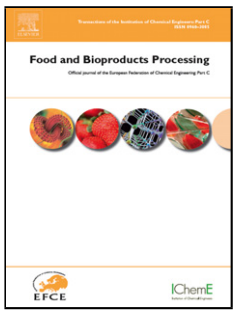

Title: Mathematical model, validation and analysis of the drying treatment on quality attributes of chicory root cubes considering variable properties and shrinkage

Authors: M.F. Balzarini, M.A. Reinheimer, M.C. Ciappini, N.J. Scenna

PII: S0960-3085(18)30529-7
DOI: https://doi.org/10.1016/j.fbp.2018.07.005
Reference: FBP 976

To appear in: *Food and Bioproducts Processing*

Received date: 1-11-2017
Revised date: 28-7-2018
Accepted date: 30-7-2018

Please cite this article as: Balzarini, M.F., Reinheimer, M.A., Ciappini, M.C., Scenna, N.J., Mathematical model, validation and analysis of the drying treatment on quality attributes of chicory root cubes considering variable properties and shrinkage.Food and Bioproducts Processing https://doi.org/10.1016/j.fbp.2018.07.005

Mathematical model, validation and analysis of the drying treatment on quality attributes of chicory root cubes considering variable properties and shrinkage

M. F. Balzarini[1,2], M.A. Reinheimer[1,3], M.C. Ciappini[2], N. J. Scenna[1,3]

[1]Centro de Aplicaciones Informáticas y Modelado en Ingeniería (CAIMI), Universidad Tecnológica Nacional, Facultad Regional Rosario (UTN, FRRo), Zeballos 1346, S2000BQA Rosario, Argentina

[2]Centro de Investigación de Tecnología de los Alimentos (CIDTA), Universidad Tecnológica Nacional, Facultad Regional Rosario (UTN, FRRo), Zeballos 1346, S2000BQA Rosario, Argentina

[3]CONICET – Consejo Nacional de Investigaciones Científicas y Técnicas, Buenos Aires, Argentina

* Corresponding author: María Agustina Reinheimer. Mailing address: *CAIMI - UTN, FRRo – Universidad Tecnológica Nacional, Facultad Regional Rosario, Zeballos 1346, S2000BQA Rosario – Argentina*. E-mail address: mareinheimer@santafe-conicet.gov.ar, Phone (+54) 341 4484909.

Highlights

- Three dimensional mathematical model to describe the drying process of chicory root (*Cichorium intibyus L.*) cubes
- Consideration of temporal variations as function of the sample humidity content for shrinkage and transfer properties
- Process representation by mathematical modeling
- Application of first principles equations and semi-empirical correlations
- Sensitive analysis for the main mass and heat transfer parameters.

Abstract

This work presents an exhaustive three dimensional mathematical model to describe chicory root cubes drying process (*Cichorium intibyus L.*) using a Fick's diffusion model considering a variable diffusion path length in three dimensions. Experimental data obtained at laboratory scale is used to validate the proposed model. Experiments are conducted using a forced convection laboratory dryer at temperatures of 60°C and 80°C and air velocities of 0.2 and 0.7 m/s to dry chicory

root cubes of 1 cm of side. Mathematical modeling is firstly used to represent the performance of the drying process with the temporal variations of the average humidity content, to determine diffusion coefficients, and afterwards, to obtain useful predictions on how the volumetric contraction of the cubes behaves under different operating conditions. The good agreements between experimental and predicted values prove that the proposed model can be applied to the precise description of experimental drying curves for chicory roots in three dimensions (3-D). In the ranges covered, the values of the effective moisture diffusivity were obtained between 5.63 10^{-5} and 8.21 10^{-5} cm^2/s. Results from the analysis of rehydration and browning aspects illustrate that drying conditions have effects on the quality attributes of the dried samples.

Keywords: 3-D; Drying; chicory roots; First-principles modeling; GAMS

Nomenclature

Symbols	
A	*empirical coefficient (Eq. (9)) (s^{-1})*
a	*dimensionless empirical coefficient (Eq. (29))*
aw	*water activity*
B	*empirical coefficient (Eq. (9)) (°K)*
b	*dimensionless empirical coefficient (Eq. (29))*
BI	*Browning index (abs.gr dm^{-1})*
C	*empirical coefficient (Eq. (9)) (g of dry matter . g of $water^{-1}$)*
c	*dimensionless empirical coefficient (Eq. (29))*
cp	*specific heat (J . g^{-1} °C^{-1})*
d	*dimensionless empirical coefficient (Eq. (8))*
D_{eff}	*effective diffusivity (cm^2 . s^{-1})*
d_{eq}	*equivalent diameter (cm)*
D_w	*diffusion coefficient of water vapor (cm^2 . s^{-1})*
e	*dimensionless empirical coefficient (Eq. (8))*
f	*dimensionless empirical coefficient (Eq. (8))*
G	*mass air flow (g . cm^{-2} . min^{-1})*
HS	*local moisture content (g of water . g of dry $matter^{-1}$)*
$\overline{HS}$	*spatially averaged moisture content (g of water . g of dry $matter^{-1}$)*
h	*convective heat transfer coefficient (J . cm^{-2} min^{-1} °C^{-1})*
k	*mass transfer coefficient (cm . min^{-1})*
K	*thermal conductivity (W . cm^{-1} °C^{-1})*
L	*characteristic length, sample semi-thickness (cm)*
P_a	*total ambient pressure (Pa)*

P_v	*partial vapor pressure (Pa)*
R	*Universal gas constant (J . °C^{-1}. mol^{-1})*
RR	*Rehydration ratio (gr absorbed water. g of dry matter $^{-1}$)*
T	*food temperature (°C)*
t	*drying time (minutes)*
Y	*specific humidity (g of vapor . g of dry air^{-1})*
x,y,z	*coordinate axes/directions*
v	*air velocity (m. s^{-1})*

Dimensionless groups

Nu	*Nusselt number (-)*
Pr	*Prandtl number (-)*
Re	*Reynolds number (-)*
Sc	*Schmidt number (-)*
Sh	*Sherwood number (-)*

Greek symbols

ΔL	*space grid with (cm)*
Δt	*temporal grid with (min)*
λ_{fg}	*Heat of vaporization (J . g water^{-1})*
μ	*viscosity (g . cm^{-1} min^{-1})*
ρ	*density (dry matter) (g . cm^{-3})*

Subscripts

a	*air*
eq	*equilibrium*
fc	*final condition*
int	*interface*
s	*food*
sur	*surface*
o	*initial condition*

1. Introduction

Chicory roots (*Cichorium intibyus L.*) are seasonal and highly perishable products, which, from an industrial point of view, require a short processing period or cold storage equipment of vast dimensions. For this reason, to enable a longer availability period for the industrial production and thus ensure the constant supply of products, it is necessary that alternatives to provide chicory root during the year be created. The drying process would then be a viable alternative to reduce water activity of raw material and, thereby, extend its usefulness.

Knowledge of the drying kinetics of biological materials is essential to the design, optimization and control of drying process (Sacilik *et al*., 2006). The use of validated simulation and optimization mathematical models are an adequate tool to define drying operating conditions with the objective

of preserving the retention of functional components, like antioxidants, for the particular case here discussed. Therefore, it is important to obtain a complete and rigorous mathematical model.

In the field of drying modeling, different kinds of mathematical models are presented. The simplest models only involve mass transfer equations (Azzouz *et al*., 2002; Hassini *et al*., 2004; Velic *et al*., 2004), assuming that the temperature gradient is too small and that it has no effect in the mass transfer rate. Most mathematical drying models found in the literature involve heat and mass transfer equations using ideal initial and boundary conditions like the equilibrium point. There is other set of works that postulate that shrinkage is negligible, which is not suitable for all biological materials (Karim *et al*., 2005; Park *et al*., 2007; Chandra Mohan *et al*., 2010; Jomlapelatikul *et al*., 2016). However, for vegetables, it is proved that the shrinkage phenomena occur (Liu *et al*., 2012; Ruiz-López, 2012; Afaghi *et al*., 2013).

Regarding to food products with high moisture content, a significant contraction during the drying is produced, which reduces the sample thickness. Therefore, constant length to calculate mass and heat transfer coefficients is not adequate. The thickness reduction occurs due to a moisture gradient within the particle that induces tensions in the microstructure, resulting in the products contraction. Furthermore, shrinkage diminishes the rate of heat transfer and spread processes which is extremely important during drying, since it produces a change in the necessary distance for the water molecules movement (Ruiz-López & García-Alvarado, 2007; Janjai *et al*., 2008; Zielinska & Markowski, 2010; Milczarek *et al*., 2011; Thuwapanichayanan *et al*., 2011).

Fick's law of diffusion is widely implemented to describe the mass transfer during drying. Many works that consider the temperature effect in the diffusional coefficient have been published (Oliveira, 2005; Oliveira *et al*., 2006; Park *et al*., 2007; Oliveira, 2009; Askari, 2013).

Probably, the work of Wang and Brennan (Wang, 1995) is one of the most extensive 1-D models in which simultaneous description of moisture and temperature profiles during the drying of potato slices considering non-constant physicochemical properties is presented. The authors also demonstrated that the shrinkage process had relevant influence on the drying behavior. Tzempelikos (Tzempelikos, 2015) presented 1-D mathematical model taking into account variable convective

coefficients and the shrinkage process during drying of cylindrical quince slices. It is important to highlight that according to the product geometry, descriptions in 2-D or 3-D are necessary to be postulated. However, few works considering 3-D mathematical models and variable coefficients are found in the literature because of the complexity of the non-linear equations which makes the solution procedure complicated and computationally demanding. Examples of unsteady tri-dimensional coupled heat conduction and mass diffusion mathematical model for the drying process of solid food but neglecting the shrinkage phenomena caused by the water movement during the diffusion process are the works of Askari and coworkers (2013), Lemus-Mondaca, and cowokers (2013).

The shrinkage process affects the size of the particulates under study, which is the visible transformation of the geometry, then, as the length and moisture content of the particle are diminished during the drying time, it is assumed that mass and heat drying coefficients vary with the moisture content and the drying time. This phenomenon has been recognized as the main factor affecting water diffusivity estimation due to the shortening of water diffusion path (Ruiz-López & García-Alvarado, 2007; Janjai *et al*., 2008; Zielinska & Markowski, 2010; Milczarek *et al*., 2011; Thuwapanichayanan *et al*., 2011).

Although, many researchers studied mass and heat transfer within chicory roots, their works were always based on the assumptions of negligible shrinkage and constant effective diffusion coefficient (Oliveira *et al*., 2006; Park *et al*., 2007; Oliveira, 2009; Brod, 2001).

The objective of this study is to develop a three-dimensional drying model which takes into account simultaneous heat and mass transfers, accompanying temporal shrinkage of the drying material and variable diffusivity along the drying process. The model was validated with experimental laboratory results run at different drying temperatures and velocities for chicory root cubes. Drying temperatures and speed effects are also studied for the transfer rates and shrinkage process. Then, quality aspects of rehydration and browning have been analyzed for all the dried samples illustrating the influence of air drying temperatures and velocities on these attributes.

2. Materials and Methods

2.1. Raw material and sample preparation

Fresh chicory roots (*Cichorium intybus L.*) were provided by a nearby farmer to the city of Rosario (Santa Fe) Argentina. The roots were washed with an aqueous solution of neutral detergent and rinsed with tap water three times. Samples of approximately 700 grams were cut into cubes with dimension of 1 cm x 1 cm x 1 cm using a special cutting tool.

2.2. Drying experiments

Drying experiments were conducted using a forced convection laboratory dryer (Tecno Dalvo, Model CHC/F /I, Argentina) at temperatures of 60°C and 80°C and air velocities of 0.2 and 0.7 m/s according to Figueira and coworkers (2003) which obtained suitable results in the drying process of chicory roots at different temperatures. Drying experiments were performed in duplicate. The samples were placed on a stainless steel mesh tray to facilitate airflow circulation.

In order to compute the moisture content, the partially dehydrated products' mass was recorded at time intervals using a digital balance with an accuracy of ± 0.01 gram. The drying process was continued until the equilibrium moisture content HSeq was reached. The equilibrium moisture content, HS_{eq}, was determined when no discernible weight change was observed for the dried samples, at that point it was assumed that the equilibrium moisture was reached.

Measurements of temperature inside and on the surface of the samples undergoing drying was carried out using a type K thermocouple with 1.5 mm diameter probe (TFA Dostman GmbH, Wertheim, Germany).

2.3 Rehydration evaluation

Rehydration ratio (RR) was used to measure the water absorption ability of dried samples. RR was determined by immersing a wire mesh with 1 g of dried chicory root cubes in 50 ml of distilled water at 30 and 100 ^{0} C temperatures. The water was drained and the samples weighed at every 5 minutes during 15 minutes and then every 15 minutes until constant weight for the samples at and 30 ^{0} C and at every 1 minute for those at 100 ^{0} C. Triplicate samples were used. RR was calculated as the ratio between rehydrated and dried sample weights.

2.4 Non – enzymatic browning index determination

Non enzymatic browning compounds solubilized in the rehydration water during the rehydration evaluation was first clarified by centrifugation at 3200x*g* for 10 min. The supernatant was diluted with an equal volume of ethanol at 95% and centrifuged again at the same conditions. Then, the browning index (BI) was determined in the clear extracts using a spectrophotometer (UV-1800, Shimatzu, Japan) at 420 nm. All measurements were done in triplicate.

2.5 Statistical analysis

The data were subjected to the analysis of variance (ANOVA) and Duncan's New Multiple Range test at a confidence level of p = 0.05 using the SPSS Statistical Analysis Program for Windows (SPSS Inc., Chicago, IL, USA).

3. Mathematical Model

To describe moisture and temperature profiles within samples during the drying process, a mathematical model is proposed considering mass and energy conservation laws under the following assumptions:

- The water diffuses to the surface of each particle according to Fick´s second law.
- Initial cubes of 1 cm of side are considered.
- Water evaporation takes place at the surface level only. Moisture movement and heat transfer are taking into account in the three dimensions.
- The moisture at the surface is at equilibrium with the drying air.
- The internal thermal resistance (chicory) is lesser than the external resistance (air), since the food thermal conductivity is larger than the fluid's. Thereby, it is considered uniform temperature distribution within the drying material.
- The shrinkage occurs on the six sides of each cube, but its shape does not change during drying.

- Homogeneous structure of the material is considered.
- Air temperature is kept constant. There is sufficient air flowrate to evaporate the internal moisture content.
- Moisture diffusivity depends on both solid moisture content and temperature.

3.1. Mass transfer Model

The equations applied to describe simultaneous heat and mass transfer in a shrinking wet chicory cube subjected to convection boundary conditions are applied and written in 3-D Cartesian coordinates, which are fixed in the geometric center of the cube. Furthermore, variable physical and thermal properties are also incorporated in the model.

A three-dimensional Fickian diffusion model of moisture transfer is applied to estimate the time evolution of the spatial distribution of the local moisture content in a chicory cube of half-thickness L during drying, which is effectively simulating 1/8th of a cube and assuming symmetrical behavior in the other 7/8ths:

$$\frac{\partial(\rho_s \times HS)}{\partial t} = \nabla\left(D_{eff} \times \nabla(\rho_s \times HS)\right) \quad (1)$$

In this model, thermo-physical properties are considered as a function of the solid temperature and moisture content. Hence, for a cube in 3-D, Equation (1) takes the following structure.

$$\frac{\partial(\rho_s \times HS)}{\partial t} = \frac{\partial}{\partial x}\left(D_{eff}\frac{\partial}{\partial x}(\rho_s \times HS)\right) + \frac{\partial}{\partial y}\left(D_{eff}\frac{\partial}{\partial y}(\rho_s \times HS)\right) + \frac{\partial}{\partial z}\left(D_{eff}\frac{\partial}{\partial z}(\rho_s \times HS)\right) \quad (2)$$

$$(t > 0; 0 < x < L_x(t); 0 < y < L_y(t); 0 < z < L_z(t)$$

where *HS* is the food moisture content at each instant of time; ρ_s is the food density; D_{eff} is the effective diffusion coefficient of the moisture content; *t* is the drying time and *L is the* characteristic length of the sample (semi-thickness).

The following initial and boundary conditions are adopted to solve Equation (2):

$$HS(x,y,z,0) = HS_o \quad (3)$$

$$(t = 0; 0 < x < L_x(t); 0 < y < L_y(t); 0 < z < L_z(t))$$

$$-D_{eff}(t) \times \left(\frac{\partial}{\partial x}(\rho_s(t) \times HS(0,y,z,t) + \frac{\partial}{\partial y}(\rho_s(t) \times HS(x,0,z,t) + \frac{\partial}{\partial z}(\rho_s(t) \times HS(x,y,0,t)\right) = 0 \quad (4)$$

$$(t = 0;\ x = 0; y = 0; z = 0)$$

$$-D_{eff}(t) \times \left(\frac{\partial}{\partial x}(\rho_s(t) \times HS(x,y,z,t)) + \frac{\partial}{\partial y}(\rho_s(t) \times HS(x,y,z,t)) + \frac{\partial}{\partial z}(\rho_s(t) \times HS(x,y,z,t))\right) =$$

$$k(t) \times \rho_a(\, Y_{int}(t) - Y_a) \quad (5)$$

$$(t > 0; x = L_x(t); y = L_y(t); z = L_z(t))$$

where

Y_a is the specific humidity in the ambient air and $Y_{int}(t)$ is the humidity at the air-food material interface. Both humidities are calculated using the following equations:

$$Y_a = \frac{0.622 \times \phi \times p_v(T_a)}{(p_a - \phi \times p_v(T_a))} \quad (6)$$

where, relative humidity, ϕ, is the ratio of partial vapor pressure P_v to the saturated vapor pressure at the same temperature and p_a is the total ambient pressure.

$$Y_{int} = \frac{0.662 \times a_w \times p_v(T_{s,sur})}{\left(p_a - a_w \times p_v(T_{s,sur})\right)} \quad (7)$$

The water activity a_w is estimated using a quadratic expression of the moisture content obtained by the adjustment of different drying experiences, reported in Table 2:

$$a_w(t) = d \times \overline{HS}(t)^2 + e \times \overline{HS}(t) + f \quad (8)$$

Equation (5) describes that a convection mechanism is considered for the mass transfer from the product surface to bulk air; where *k* is the external mass transfer coefficient.

It is accepted that the effective diffusion coefficient can be described by an exponential form considering the moisture dependence and the Arrhenius temperature influence (Karathanos, 1990; Parti & Dugmaniscs, 1990; Wang & Brennan, 1995; Białobrzewski & Markowski, 2004; Ruiz-López et al., 2004), according to Equation (9), in which A, B and C are fit parameters determined during the model optimization:

$$D_{eff}(t) = A \times exp\left(\frac{-B}{(273.15+T_s)}\right) \times exp(C \times \overline{HS}(t)) \quad (9)$$

Therefore, the effective moisture diffusion coefficient, D_{eff} (Equation 9), is a function of the solid temperature (T_s) and the moisture content during the drying process. Also, all these variables are dependent of the drying time.

The mass transfer coefficient, *k*, used in Equation (5), is determined using the Sherwood number, *Sh*, calculated from the dimensionless equation reported by Mills (1995) in conjunction with Equations from 11 to 16:

$$Sh(t) = \frac{d_{eq(t)} \times k_{(t)}}{D_w} = 2 + 0.6 \times Re(t)^{0.5} \times Sc^{0.33} \quad (10)$$

$$\mu_a = \frac{0.000001 \times 1.4592 \times ((T_a+273)^{1.5})}{(109.10+(T_a+273))} \quad (11)$$

$$\rho_a = \frac{M_a \times P_a}{R \times (T_a+273)} \quad (12)$$

$$G_a = \frac{P_a \times v \times M_a}{R \times (T_a + 273)} \quad (13)$$

$$d_{eq}(t) = L_x(t) \times \sqrt{\left(\frac{6}{\pi}\right)} \quad (14)$$

$$Re(t) = \frac{d_{eq}(t) \times G_a}{\mu_a} \quad (15)$$

$$Sc = \frac{\mu_a}{\rho_a \times D_w} \quad (16)$$

The estimation of the average moisture content at each instant of time in the chicory root cubes is obtained by integrating local moisture content over the volume. Specifically, the average moisture content is expressed as stated Equation (17), which can be evaluated using the Trapezium rule.

$$\overline{HS}(t) = \frac{\int_0^V HS(x,y,z,t)dV}{\int_0^V dV}, t \geq 0 \quad (17)$$

3.2. Heat Transfer Model

In addition to mass transfer, simultaneous heat transfer occurs during drying of foodstuffs, which is modeled as non-steady heat conduction within the product as (Białobrzewski & Markowski, 2004):

$$\frac{\partial(\rho_s \times cp_s \times T_s)}{\partial t} = \frac{\partial}{\partial x}\left(K_s \times \frac{\partial}{\partial x} T_s\right) + \frac{\partial}{\partial y}\left(K_s \times \frac{\partial}{\partial y} T_s\right) + \frac{\partial}{\partial z}\left(K_s \times \frac{\partial}{\partial z} T_s\right) \quad (18)$$

$$(t > 0; 0 < x < L_x(t); 0 < y < L_y(t); 0 < z < L_z(t)$$

where, T_s is the food temperature, cp_s is the food specific heat and K_s is the food thermal conductivity.

The following initial and boundary conditions are adopted to solve Equation (21):

$$T_s(x, y, z, 0) = T_{s_o} \quad (19)$$

$$(t = 0; 0 < x < L_x(t); 0 < y < L_y(t); 0 < z < L_z(t)$$

$$-K_s(t)\left(\frac{\partial}{\partial x}T_s(0,y,z,y)+\frac{\partial}{\partial y}T_s(x,0,z,t)+\frac{\partial}{\partial z}T_s(x,y,0,t\right)=0 \quad (20)$$

$(t=0;\ x=0;y=0;z=0)$

$$K_s(t)\times\left(\frac{\partial}{\partial x}T_s(x,y,z,t)+\frac{\partial}{\partial y}T_s(x,y,z,t)+\frac{\partial}{\partial z}T_s(x,y,z,t)\right)=h\,(t)\times\left(T_a\ -T_s(x,y,z,t)\right)-\ k(t)\times\rho_a(\,Y_{int}(t)-Y_a)\times\lambda_{fg}$$

(21)

$(t>0;x=L_x(t);y=L_y(t);z=L_z(t))$

In Equation (21), *h,* is the convective heat transfer coefficient and, λ_{fg}, is the heat of vaporization. In this equation, the term on the left side refers to the heat conducted from the outer surface to the inside of the body. The first term on the right side is the heat penetrating from the environment to the solid body by convection, and the second term on the right side denotes the evaporation heat.

The heat transfer coefficient, *h*, for the chicory roots cubes is determined using Nusselt number, *Nu,* calculated from the dimensionless equation reported by Pohlhausen (1921) for Re < 5.10^5 and Pr > 0.6.

$$Nu(t)=\frac{h_m\,(t)\times deq(t)}{k_a}=0.332\times Re(t)^{0.5}\ \times Pr^{0.33} \quad (22)$$

$$Pr=\frac{cp_a\times\mu_a}{k_a} \quad (23)$$

The thermophysical properties, specific heat, cp_s, and thermal conductivity, k_s are estimated using the correlations of Choi and Okos (1986) and Singh and Heldman (1993), respectively:

$$Cp_s(t)=0.84+3.55\times\frac{\overline{HS}(t)}{1+\overline{HS}(t)} \quad (24)$$

$$K_s(t)=1.418\times10^{-3}\ +4.93\times10^{-3}\ \times\frac{\overline{HS}(t)}{1+\overline{HS}(t)} \quad (25)$$

2.3. Model Solution Strategy

Equations (2-4, 18-21) are discretized using the central finite difference method (CFDM) and the implicit method. This scheme, which has first-order accuracy in time and second-order accuracy in space, is unconditionally stable and convergent. Equations 26 and 27 define the spatial and temporal variations, respectively, with M = 9 and N = 32. The values of *M* and *N* have been previously proved and ensure the stability of the solution with the lower computational demand.

$$\Delta Li(t) = \frac{Li(t)}{M} \tag{26}$$

$$\Delta t = \frac{t_{fc}}{N} \tag{27}$$

This work is the first step of a challenging project, which consists of the model-based optimization of a full-scale facility to obtain extracts with antioxidants properties. Therefore, this mathematical model will be the basis of the optimization model for the drying unit operation. The proposed non-linear programming model was implemented in GAMS (General Algebraic Modeling System) and solved using CONOPT (Singh & Heldman, 1993), an algorithm based on the reduced gradient method.

Figure 1 summarizes the scheme of work. As first step, the model is used to estimate the parameters of the diffusion coefficient (eq. (9)) by the application of the objective function (*OF*) based on the minimization of the mean-square error (MSE) of our experimental and predicted data points of moisture content and size contraction and presented in eq. (31). Here, the goal is to evaluate the performance of the model and the implemented correlations used to describe the heat and mass transfer during drying. After that, *OF* is again implemented in order to obtain the polynomial coefficients that describe the contraction as a function of the moisture content, according to the following equation:

$$\frac{V(t)}{V_o} = a \times \overline{HS}(t)^2 + b \times \overline{HS}(t) + c \tag{28}$$

where a, b and c are the estimated parameters of the optimization model at different drying conditions.

$$V(t) = 2\left(L(t)\right)^3 \quad (29)$$

where L(t) is the sample semi-thickness and it is considered that the contraction is homogeneous in all the cube faces:

$$L_x(t) = L_y(t) = L_z(t) = L(t) \quad (30)$$

$$OF = Min\{MSE\} = Min\left\{\frac{1}{N}\left(\sum_{t_o}^{t_f}\left(\overline{HS}_{exp}(t) - \overline{HS}(t)\right)^2\right) + \frac{1}{N}\left(\sum_{t_o}^{t_f}\left(L_{exp}(t) - L(t)\right)^2\right)\right\} \quad (31)$$

It is interesting to remark that the solution of the minimization problem is quite close to the real behavior of the shrinkage process. This is achieved only using well proved correlations about all the other critical parameters of the whole drying process.

Well proved correlations reported in the literature are adopted to predict heat and mass transfer coefficients in order to reduce the model degrees of freedom and facilitate the resolution of the NLP model.

Figure 1 summarizes different variables, parameters and experimental input data required to solve the model. In this way, the model can predict the behavior of the shrinkage process considering different operating conditions. As summary, the implemented model estimates the parameter of the diffusion coefficients (*A*, *B* and *C* of eq. (9)), then these coefficients are included in the model and the polynomial coefficients of the contraction equation (*a*, *b* and *c* of eq. (28)) are calculated.

3.4. Parameters

The main model parameters classified as physicochemical properties and operating conditions are listed in Table 1 and Table 2.

4. Results and discussion

4.1. Performance of the model

Table 3 presents the corresponding value of the Mean Square error (MSE) for the implemented model. From the results, it is concluded that MSE are low for both cases, being the

model satisfactory to describe the drying process as well as the shrinkage process and obtain the diffusion and shrinkage parameters.

4.2. Drying Kinetics

Figure 2 and 3 show comparison of the experimental and predicted average moisture content profiles carried out at different air drying temperatures and velocities. It is observed that the proposed model accurately describes the drying kinetics for all the experiments.

The drying time to reach the equilibrium moisture content and R^2 values for all the experimental runs are listed in Table 4. It is observed from both figures that the air temperatures exercise a noticeable impact on drying rates. As expected higher drying temperatures lead to higher rates of removal moisture and therefore shorter drying times due to the higher temperature differences between the sample and the drying medium.

The loss of moisture is very fast during the beginning of the drying process because of the large difference between the moisture content of the chicory root and the moisture content corresponding to equilibrium with the dry air. Initially, the gradient of moisture content is high. The free moisture being removed increases as the rate of convection heat and mass transfer is increased. This initial change of the moisture content is caused by a variation of the surface temperature. The product temperature is gradually increased during this period. In the falling rate drying period, moisture in chicory roots migrated from the inside to the surface of each sample because the rate of moisture movement is controlled by moisture diffusion rate through the product. At the end of the dehydration process, the moisture profile becomes flatten and tends to lower moisture levels until reaching the equilibrium moisture content of the chicory roots.

4.3. Sample temperature evolution

The average experimental and estimated temperature evolutions for chicory root samples are compared in Figure 4. Temperature vales are not fitting data points in the model. Therefore, as can be observed in Figure 4, the prediction presents high accuracy.

At the beginning of drying process (t < 150 minutes), the temperature of the food increases rapidly due to the difference between air and food temperatures; at this time, most of the heat is used to evaporate water at the surface. About 75% of the water has evaporated. As the heating period progresses, the increment in temperature attains an almost uniform profile in which it can be considered constant (150< t < 630 minutes) and moisture becomes near to the equilibrium values. Most of the heat is used to raise the temperature of the food until reach the drying air temperature (Ruiz-López & García Alvarado, 2007).

4.4. Effective moisture diffusivities

Estimated water effective diffusivities are plotted in Figure 5. The diffusion coefficient depends on sample temperature and moisture, and the estimated parameters of the Eq.(9) are A=1.008 (1/s), B=3205.42 (K) and C=0.058 (g d.m./g water). Water diffusion coefficient increases with the increment of drying air temperature as shown Figure 5. As expected, the use of higher drying temperatures promotes a higher water mobility in food system (Ruiz-López, 2012) and thus increases the effective diffusivity of mass transfer. Despite the fact that higher temperature than 80°C are not appropriate due to the thermal degradation of antioxidant components. Furthermore, the effective diffusivity increases as air-drying velocity increases. However, the air velocity has not shown a significant influence on the diffusion coefficient for both drying temperatures.

As indicated Figure 6, a decrease in the value of the diffusivity is evidenced as the drying process progresses due to the temporal moisture reduction. In the final drying period (t> 200 minutes), the diffusivity takes a constant value corresponding to the diffusivity for the equilibrium moisture. Similar results were obtained by Rahman and coworkers (2007), who showed that the diffusivity is high at the beginning of drying and then was kept constant at the final drying period.

Analyzing the results, it is fundamental to take into account particle shrinkage, either with a variable L(t) in the mass transfer model equations Eqs. (1)-(5) in order to obtain representative moisture transfer phenomena.

4.5. Shrinkage

Experimental and predicted contraction data obtained during convective drying chicory roots cubes as a function of the average moisture content at different conditions are plotted in Figure 7. The shrinkage of the product is shown by the change in the volume of the sample. This model allows to reproduce in a very satisfactory way the measured values.

At early drying times (corresponding to $\overline{HS}$ greater than 2.5 g water/ g d.m.), small size variations are evidenced on the cube samples, corresponding to the constant rate period. In this period, the main process is the surface water evaporation. However, during the falling rate period, ($\overline{HS}$ lower than 2.5 g water/ g d.m.), large volume variations are observed in all the experimental runs associated with the water molecular movement during the diffusion process. Then, at the end of the drying process (approximately $\overline{HS}$ lower than 0.5 g water / g d.m.), small contraction is evidenced because of the low moisture transport within the solid. It was observed that the degree of shrinkage of chicory roots during low temperature drying is greater than with high temperature drying, due to surface case hardening at higher temperatures, which restrains the size reduction.

The vegetables' contraction results in their own stiffening, a phenomenon which is produced in some drying processes. As the food surface dries, which occurs in a larger rate than its nucleus' dries, the internal tensions develop internal fissures (Aguilera & Stanley, 1999). The non-volatile compounds flow with the water by diffusion. Then, they precipitate in the product's surface and shape a rind, which maintains the food's dimensions from then on.

Some authors reported the shrinkage process as a linear function of the sample moisture content (Białobrzewski, 2006; Mihoubi & Bellagi, 2008; Bacelos & Almeida, 2011). However, in this work, it is found that the relation between the volume ratio contraction and the moisture content is almost a second-order polynomial trend curve. These results are in agreement with the ones reported by other authors (Panyawong & Devahastin, 2007; Yan, 2008; Ruiz-López, 2012; Afaghi, 2013). Hence, the Equation (28) is adopted to represent the relationship between the volume ratio contraction and the average moisture content of chicory root cubes at different conditions of drying. The obtained values and the adjustment coefficients are listed in Table 5.

4.6. Mass and heat transfer coefficients

The variation of mass and heat transfer coefficients for different velocities and temperatures, calculated with equations (10) and (22), respectively, are shown in Figures 8 and 9. It can be observed that both coefficients increase with the raise of the air temperature and velocity, having greater rate transfers for the mass and heat forced convection. From the figures, it can be appreciated that the changes in velocity had more effect than the changes in temperature.

4.7. Prediction and confidence bands

Figure 10 presents the confidence band (CB) and prediction band (PB) for moisture content against drying times. The PB is the region where 95% of the experimental data points are expected to be, whereas it is here observed that all obtained observations fall within. Likewise, the CB is the region where 95% of the regression lines are expected to be, and contains more than 50% of the experimental values for all the experiences here reported. Both obtained CB and PB are well adjusted to the experimental data points, therefore increasing the confidence on the values predicted for the model. Normal probability plots of residuals are also presented in Figure 11 for the experimental runs of chicory root drying at 60 and 80ºC. As the data points are equally distributed above and below the line, it is verified that they are normally distributed and no unwanted trends or correlations among the data points exist (skewness, presence of an undefined variable, outliers, among others).

4.8. Sensitivity analysis

In this section, parameters from empirical correlations implemented in the proposed model are varied between -30% and 30%, in order to analyze their impact to estimate the required drying time in order to achieve the equilibrium moisture content. Figure 12 presents spider diagrams for the drying process of chicory root cubes at 60 and 80ºC and both drying velocities. It is noted that similar trends were observed for all the experimental runs. As can be appreciated in all figures, the water diffusion coefficient exerts the larger impact over the final moisture content, as it is the controlling

drying process. The sensitivity of this parameter is high, indicating that, moment to moment, the moisture content is highly dependent on the diffusion coefficient. In terms of parameter estimation, this indicates that minor changes in the value of this parameter affect the model. Therefore, the rest of the mass and heat transfer parameters have little effect on the final moisture content. The results here obtained are in agreement with the results presented by da Silva (2009), who exposed that the diffusion is the controlling step of the process, in which higher diffusion coefficients were obtained for higher drying temperatures and velocities.

4.9. Shrinkage analysis and prediction

Considering the mathematical model as a prediction tool for design purposes, it is important the estimation of the shrinkage process and volume contraction as a function of the main operating variables (air temperature and velocity). This predictive tool could have a valuable implementation in some practical cases in which the contraction must be carefully controlled in order not to alter the visual characteristics of the dried samples. In previous sections, the contraction process of shrinkage has been analyzed as a function of the time and moisture changes during the drying process. But, for the analysis of the final dried product, it is preferable to evaluate in a predictive way the contraction regarding the drying operating conditions. Therefore, in this section a surface analysis of the final contraction (associated at the equilibrium moisture) is presented covering the range of the operating conditions validated in the model, that is air temperatures from 60 to 80 ^{0} C and air velocities from 0.2 m/s to 0.7 m/s. The data of final contraction obtained from different combination of air temperatures and velocities were fitted to different response surfaces (linear, quadratic, full quadratic). The best fitted corresponds to a linear response surface regression, taking the following equation form (Adj R^2=0.8703 and R^2=0.8284):

$$\frac{V}{V_0} = -0.268 + 0.00665 \cdot T_a - 0.0907 \cdot v \quad (29)$$

The model suitability is tested by the implementation of the R^2 adjusted equations and the sequential squares sums for each regression coefficient of the RSM model. The ANOVA results are

presented in Table 6. F-value is a way of analysis of the variance between the regression of the square error and the real mean error. High F values mean that the response variations can be explained by the obtained regression equation. The purpose of the R^2 adjusted values is to analyze the model adequacy. Here, R^2 adjusted model is consistent with R^2 values, therefore the predicted values correlate with the experimental ones. The ANOVA for the linear model of V/V0 demonstrate that it is significant ($p<0.05$).

Surface response plots allows one to visualize the effect of the independent variables on the dependent variables. Figure 13 shows that the final volume contraction (V/V_0) increases for lower air drying temperatures and velocities. At the studied operating conditions ranges, the air velocity is insignificant ($p>0.05$) having no influence on the volume contraction, but it is clear that the studied velocity range is not so wide. On the other hand, the air temperature is highly significant ($p<0.01$).

4.10 Effect of the drying treatment on the rehydration ratio

Rehydration is an important attribute to evaluate dried foodstuffs. The RR is directly related with the drying conditions (air drying temperature and velocity). Different physical and chemical changes are observed depending on the drying treatment (Noshad et al., 2012). The rehydration curves of chicory roots samples dried at different conditions are shown in Figure 14, which have the tendency to an asymptotic value for all drying conditions. Higher RR are shown for lower air drying temperature and velocity. It is evidenced that more severe drying treatment (higher air temperature and velocity) has a negative effect influence on RR, which could be associated to the stronger surface case hardening associated with less contraction. Lower air temperature and velocity causes less shrinkage with a porous structure that provides better rehydration process. These results are in agreement with those obtained by Giri and Prassat (2007) and Apati and coworkers (2010).

4.11 Effect of the drying treatment on the browning index

Browning is another important quality attribute for dried products. It was proven that higher drying temperatures and velocities significantly accelerate deterioration of color samples because of non-enzymatic browning reactions (Xiao, 2014). Figure 15 shows the BI for each drying treatment and rehydration evaluation at 30 and 100. The results clearly evidence how BI increases with the air temperature and velocity and BI is not influenced by the rehydration treatment because it is affected by the drying conditions.

5. Conclusions

A complete three dimensional mathematical model to simultaneously describe mass and heat transfer of the drying process of chicory root cubes has been presented. The model considers a variable effective diffusion coefficient depending on the changes of the sample moisture content and temperature. It is developed using first principles equations through DAEs and semi-empirical correlations.

The moisture distribution and the temperature development are modeled for the drying process of chicory root cubes in a conventional air drier with forced air flows at different temperatures and velocities. High accuracy is evidenced between experimental and simulated data. The proposed methodology represents a feasible way of estimation of the shrinkage process under the analyzed range of the operating variables for the cubes.

From the analysis of the results, it is observed that the effective diffusion coefficient and the solid contraction is strongly more influenced by the change in the drying temperature than the air drying velocity. On the other hand, heat and mass transfer coefficients take higher values by the increase in the air drying velocity than the temperature.

It is thus concluded that the moisture variation and contraction phenomenon must be considered during the drying process to accurately describe moisture transfer process. In addition, the developed model can be used as a useful tool to improve the operational efficiency of the drying stage of food products such as chicory or other vegetables in which the shrinkage process is a quality and control variable of interest. A further work will be focused on comparing quality aspects between conventional and vacuum drying.

Acknowledgments

The authors kindly acknowledge the financial support of the Universidad Tecnológica Nacional (UTN) and the Consejo Nacional de Investigaciones Científicas y Técnicas (CONICET) of Argentina.

References

Afaghi, N., Motlagh, A.M., Seiedlou, S.S., Hasanpour, A., 2013. Simulation shrinkage and stress generated during convective drying of carrot slices. International Journal Advanced Biological Biomedical Research. 12 (1), 1660-1668.

Aguilera, J.M., Stanley, D.W., 1999. Microstructural principles of food processing and engineering; second ed., Springer Science & Business Media: Maryland.

Apati, G.P., Furlan, S.A., Laurindo, J.B., 2010. Drying of Oyster Mushroom. Brazilian Archives of Biology and Technology. 53(4), 945-952.

Askari, G.R., Emam-Djomeh, Z., Mousavi, S.M., 2013. Heat and mass transfer in apple cubes in a microwave-assisted fluidized bed drier. Food and Bioproducts Processing. 91, 207-215.

Azzouz, S., Guizani, A., Jomaa, W., Belghith, A., 2002. Moisture diffusivity and drying kinetic equation of convective drying of grapes. Journal of Food Engineering. 55, 322-330.

Bacelos, M.S., Almeida, P.I.F., 2011. Modelling of drying kinetic of potatoes taking into account shrinkage. Procedia Food Science. 1, 713-721.

Białobrzewski, I., Markowski, M., 2004. Mass transfer in the celery slice: effects of temperature, moisture content, and density on water diffusivity. Drying Technology. 22 (17), 1777-1789.

Białobrzewski, I., 2006. Simultaneous Heat and Mass Transfer in Shrinkable Apple Slab during Drying. Drying Technology. 24(5), 551-559.

Brod, F.P.R., Park, K.J., Oliveira, R.A., 2001. Secagem de raiz de chicória em um secador convectivo. In: Congreso Brasileiro de Engenharia Agrícola, 30. Foz do Iguaçu-PR. Anais, Foz do Iguaçu-PR: SBEA.

Chandra Mohan, V. P., Talukdar, P., 2010. Three dimensional numerical modeling of simultaneous heat and moisture transfer in a moist object subjected to convective drying. International Journal of Heat and Mass Transfer. 53, 4638-4650.

Choi, Y., Okos, M., 1986. Effects of temperature and composition on the thermal properties of foods. Food Engineering and Process Application. 1, 93-116.

Da Silva, C.K.F., Da Silva, Z.E., Mariani, V.C., 2009. Determination of the diffusion coefficient of dry mushrooms using the inverse method. Journal of Food Engineering. 95, 1-10.

Drud, A., 1992. CONOPT – a large scale GRG code. ORSA Journal on Computing. 6, 207-216.

Figueira, G.M., Park, K.J., Brod, F.P.R., Honório, S.L., 2003. Evaluation of desorption isotherms, drying rates and inulin concentration of chicory roots (Cichorium intybus L.) with and without enzymatic inactivation. Journal of Food Engineering. 63, 273-280.

Giri, S.K., Prasad, S., 2007. Drying kinetics and rehydration characteristics of microwave-vacuum and convective hot-air dried mushrooms. Journal of Food Engineering. 78, 512–521.

Hassini, L., Azzouz, S., Belghith, A., 2004. Estimation of the moisture diffusion coefficient of potato during hot air drying, In: Proceedings of the 14th International Drying Symposium (IDS-2004), São Paulo, Brazil, August 22-25, 1488-1495.

Janjai, S., Lamlert, N., Intawee, P., Mahayothee, B., Haewsungcharern, M., Bala, B.K., Müller, J., 2008. Finite element simulation of drying of mango. Biosystems Engineering. 99 (4), 523-531.

Jomlapelatikul, A., Wiset, L., Duangkhamchan, W., Poomsa-ad, N., 2016. Model-based investigation of heat and mass transfer for selecting optimum intermediate moisture content in stepwise drying. Applied Thermal Engineering. 107, 987-993.

Karathanos, V. K., 1990. Water diffusivity in Starches at Extrusion Temperatures and Pressures, Ph. D. thesis, Rutgers University, New Brumswick, NJ.

Karim, M.A., Hawlader, M.N.A., 2005. Mathematical modelling and experimental investigation of tropical fruits drying. International Journal of Heat and Mass Transfer. 48, 4914-4925.

Liu, G., Chen, J., Liu, M., Wan, X., 2012. Shrinkage, porosity and density behaviour during convective drying of bio-porous material. Procedia Engineering. 31, 634-640.

Lemus-Mondaca, R.A., Zambra, C.E., Vega-Gálvez, A., Moraga, N.O., 2013. Coupled 3D heat and mass transfer model fon numerical analysis of drying process in papaya slices. Journal of Food Engineering. 116, 109-117.

Mihoubi, D., Bellagi, A., 2008. Two-dimensional heat and mass transfer during drying of deformable media. Applied Mathematical Modelling. 32, 303-314.

Milczarek, R.R., Dai, A.A., Otoni, C.G., McHugh, T.H., 2011. Effect of shrinkage on isothermal drying behavior of 2-phase olive mill waste. Journal of Food Engineering. 103 (4), 434-441.

Mills, A. F., 1995. Basic Heat and Mass Transfer. Massachusetts, Irwin.

Noshad, M., Mohebbi, M., Shahidi, F., & Mortazavi, S. A., 2012. Kinetic modeling of rehydration in air-dried quinces pretreated with osmotic dehydration and ultrasonic. Journal of Food Processing and Preservation. 36, 383-392.

Oliveira, R., 2005. Effect of chicory roots of drying in obtaining inulin. Ph. D. thesis, Campinas University UNICAMP, Campinas, San Pablo, Brazil.

Oliveira, R.A., Oliveira, W.P., Park, J.K., 2006. Determination of effective diffusivity of chicory root. Engenharia Agricola. 26 (1), 181-189.

Oliveira, R.A., 2009. Estudo da secagem em dois tipos de secadores: avaliação dos parámetros operacionais e comportamento do material seco. Ph. D. thesis, Agrícola da Universidade Estadual de Campinas. Campinas, SP, Brazil.

Panyawong, S., Devahastin, S., 2007. Determination of deformation of a food product undergoing different drying methods and conditions via evolution of a shape factor. Journal of Food Engineering. 78, 151-161.

Park, K. J., Oliveira, R.A., Brod, F.P.R., 2007. Drying operational parameters influence on chicory roots drying and inulin extraction. Food and Bioproducts Processing. 85(3), 184-192.

Parti, M., Dugmaniscs, I., 1990. Diffusion coefficient for corn drying. Transactions of the ASAE. 33 (5), 1652-1656.

Pohlhausen, E., 1921. Der Wármeaustaush zwischen festen Kôrpern and Flûssigkeiten mit Kleiner Reibung und Kleiner Wârmeleitung. ZAAM. 1, 115-121.

Rahman, M. S., Al-Marhubi, I., Al-Mahrouqi, A. M., 2007. Measurement of glass transition temperature by mechanical (DTMA), thermal (DSC and MDSC), water diffusion and density method: a comparison study. Chemical Physics Letters. 440, 372-377.

Ruiz-López, I.I., Córdova, A.V., Rodriguez-Jimenes, G.C., García-Alvarado, M.A., 2004. Moisture and temperature evolution during food drying Effect of variable properties. Journal of Food Engineering. 63, 117-124.

Ruiz-López, I.I., García-Alvarado, M.A., 2007. Analytical solution for food-drying kinetics considering shrinkage and variable diffusivity. Journal of Food Engineering. 79 (1), 208-216.

Ruiz-López, I.I., 2012 Analytical model for variable moisture diffusivity estimation and drying simulation of shrinkable food products. Journal of Food Engineering. 108, 427-435.

Sacilik, K., Elicin, A.K., Unal, G., 2006. Drying kinetics of Üryani plum in a convective hot-air dryer. Journal of Food Engineering. 76 (3), 362-368.

Singh, R.P., Heldman, D.R., 1993. Introduction to Food Engineering, second ed., Academic Press, Inc., San Diego, California.

Thuwapanichayanan, R., Prachayawarakorn, S., Kunwisawa, J., Soponronnarit, S., 2011. Determination of effective moisture diffusivity and assessment of quality attributes of banana slices during drying. LWT – Food Science and Technology. 44 (6), 1502-1510.

Tzempelikos, D.A., Mitrakos, D., Vouros, A.P., Ardakas, A.V., 2015. Numerical modeling of heat and mass transfer during convective drying of cylindrical quince slices. Journal of Food Engineering. 156, 10-21.

Velic, D., Planinic, M., Tomas, S., Bili, M., 2004. Influence of airflow velocity on kinetics of convection apple drying. Journal of Food Engineering. 64, 97-102.

Wang, N.; Brennan, J.G., 1995. Changes in structure, density and porosity of potato during dehydration. Journal of Food Engineering. 24, 47-60.

Wang, N., Brennan, J.G., 1995. A mathematical of simultaneous heat and moisture transfer during drying of potato. Journal of Food Engineering. 24, 61-76.

Xiao, H.W., Law, C., Sun, D.W., Gao, Z.J., 2014. Color change kinetics of American ginseng (*Panax quinquefolium*) slices during air impingement drying. Drying Technology. 32, 418–427.

Yan, Z., Sousa-Gallagher, M.J., Oliveira, F.A.R., 2008. Shrinkage and porosity of banana, pineapple and mango slices during air-drying. Journal of Food Engineering. 84, 430-440.

Zielinska, M., Markowski, M., 2010. Air drying characteristics and moisture diffusivity of carrots. Chemical Engineering and Processing. 49 (2), 212-218.

List of figure captions

Figure 1. Summary of the mathematical process model for representing the drying kinetics of chicory root cubes

Figure 2. Experimental and predicted variation of moisture content with time at v_1 (0.2 m/s)

Figure 3. Experimental and predicted variation of moisture content with time at v_2 (0.7 m/s)

Figure 4. Temperature evolution in material for drying v_1 (0.2 m/s) and v_2 (0.7 m/s)

Figure 5. Water diffusion coefficients within samples at v_1 (0.2 m/s) and v_2 (0.7 m/s)

Figure 6. Temporal changes in the effective water diffusion coefficients at v_1 (0.2 m/s) and v_2 (0.7 m/s)

Figure 7. Experimental and calculated sample shrinkage at v_1 (0.2 m/s) and v_2 (0.7 m/s) implementing Eq. (28)

Figure 8. Estimated mass transfer coefficients at v_1 (0.2 m/s) and v_2 (0.7 m/s)

Figure 9. Estimated heat transfer coefficients at v_1 (0.2 m/s) and v_2 (0.7 m/s)

Figure 10. Confidence and prediction bands of moisture variation at v_1 (0.2 m/s) and v_2 (0.7 m/s)

Figure 11. Normal probability plots of residuals for drying at (60 and 80) ºC and v1 (0.2 m/s)

Figure 12. Sensitivity analysis for the required drying time to achieve the equilibrium moisture at v1 (0.2 m/s) and v2 (0.7 m/s)

Figure 13. Surface response of the solid volume contraction as a function of the drying temperature and velocity

Figure 14. Effect of drying treatment on rehydration ratio (RR) of chicory roots for rehydration at 30 ^{0} C and 100 ^{0} C. Different letters in the same column indicate that values are significantly different (p-value < 0.05).

Figure 15 Browning index of the dried samples. Different letters in the same column indicate that values are significantly different (p-value < 0.05).

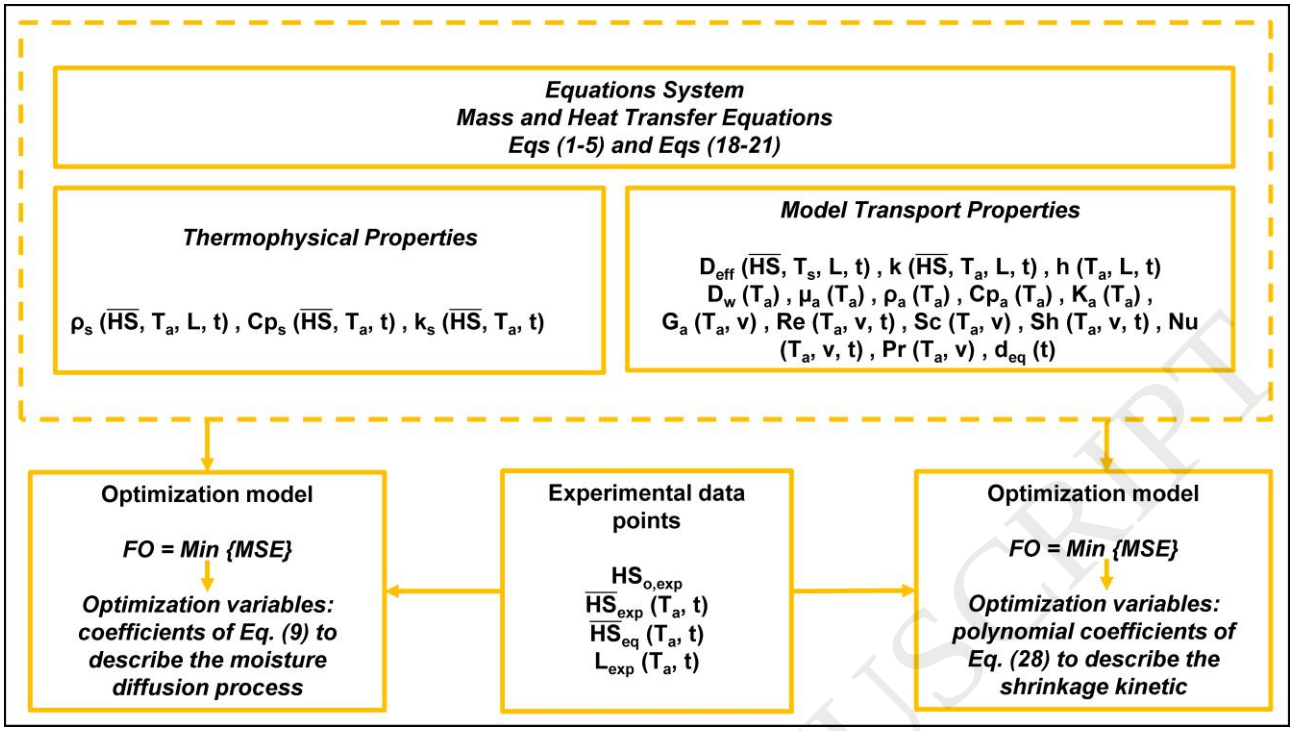

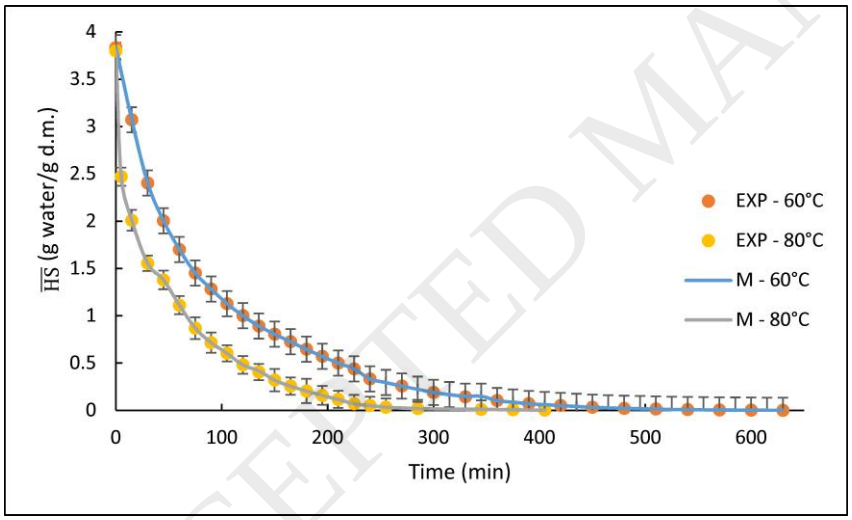

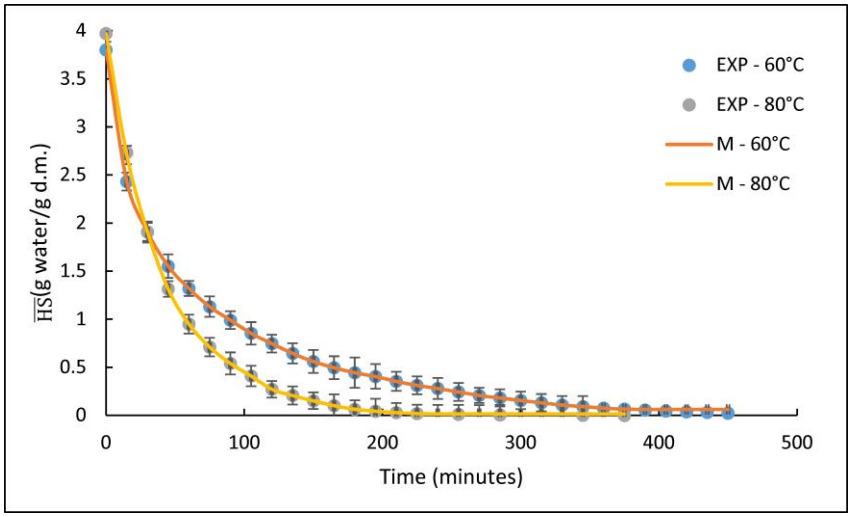

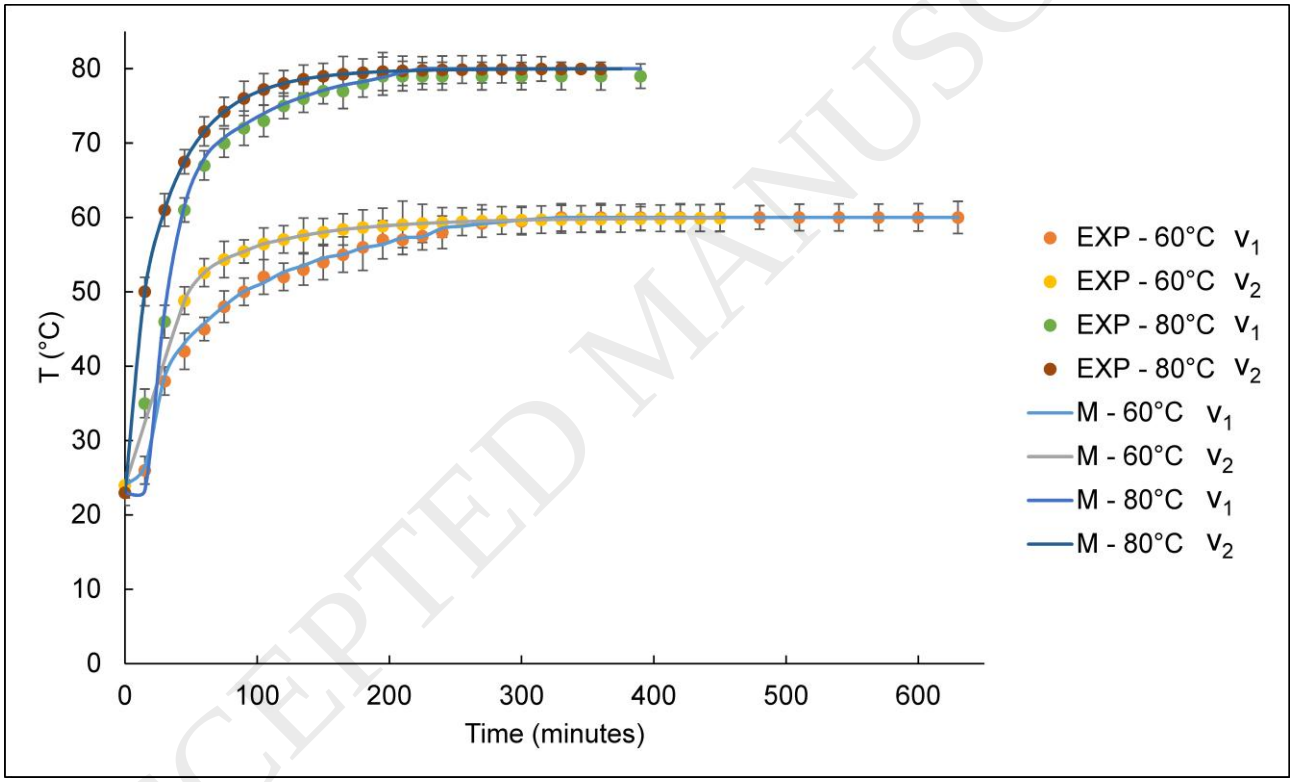

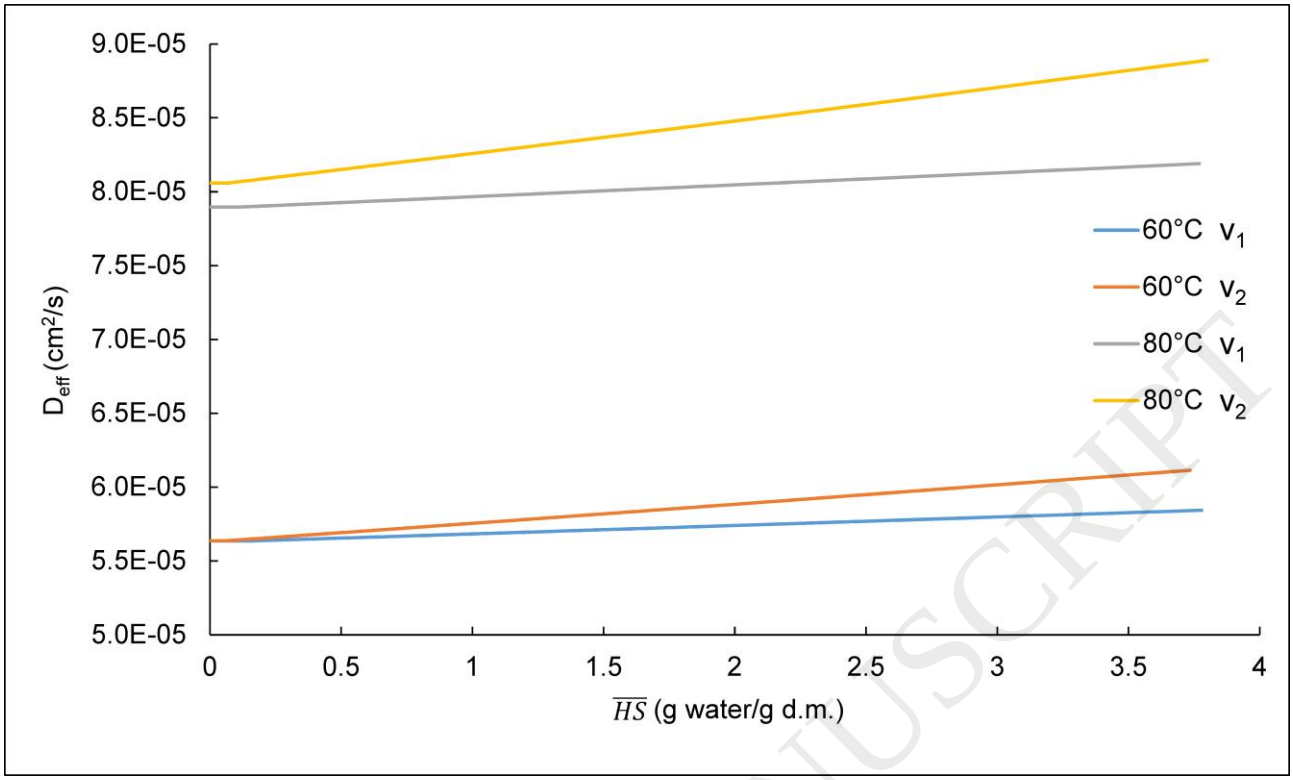

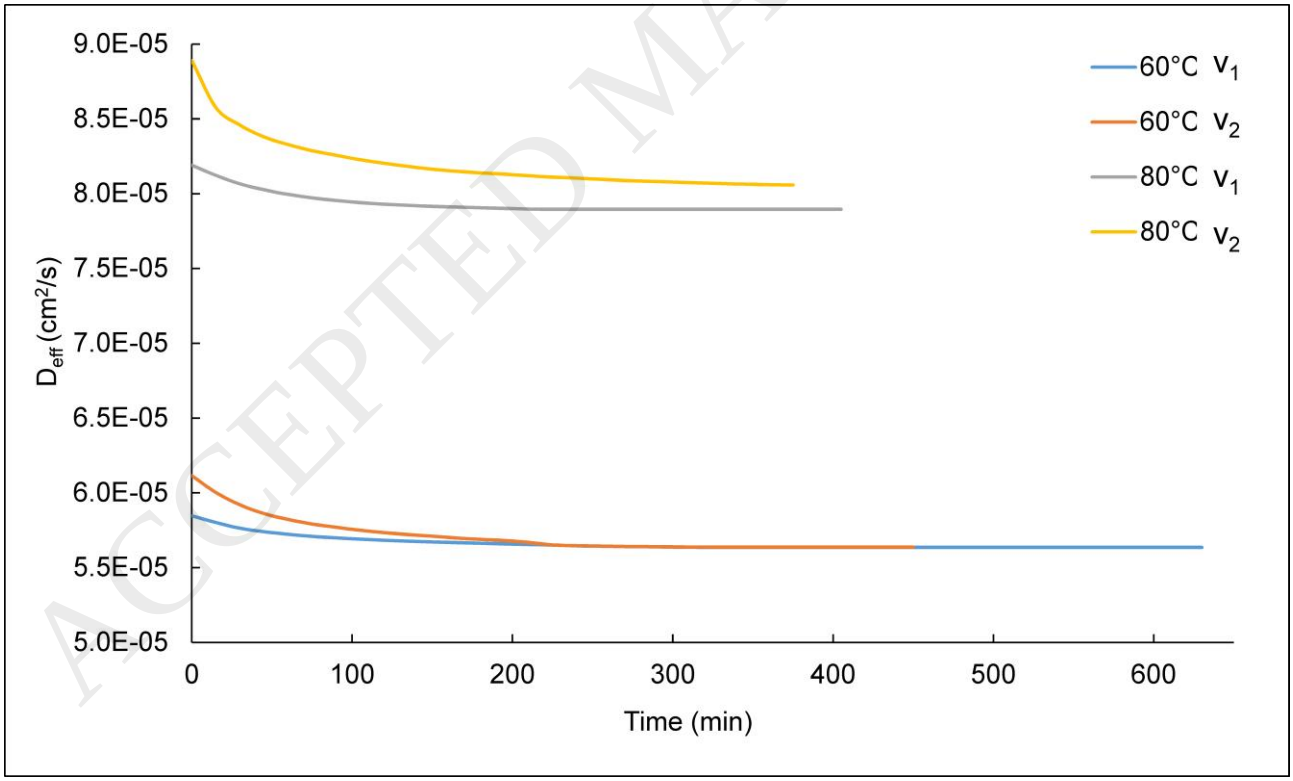

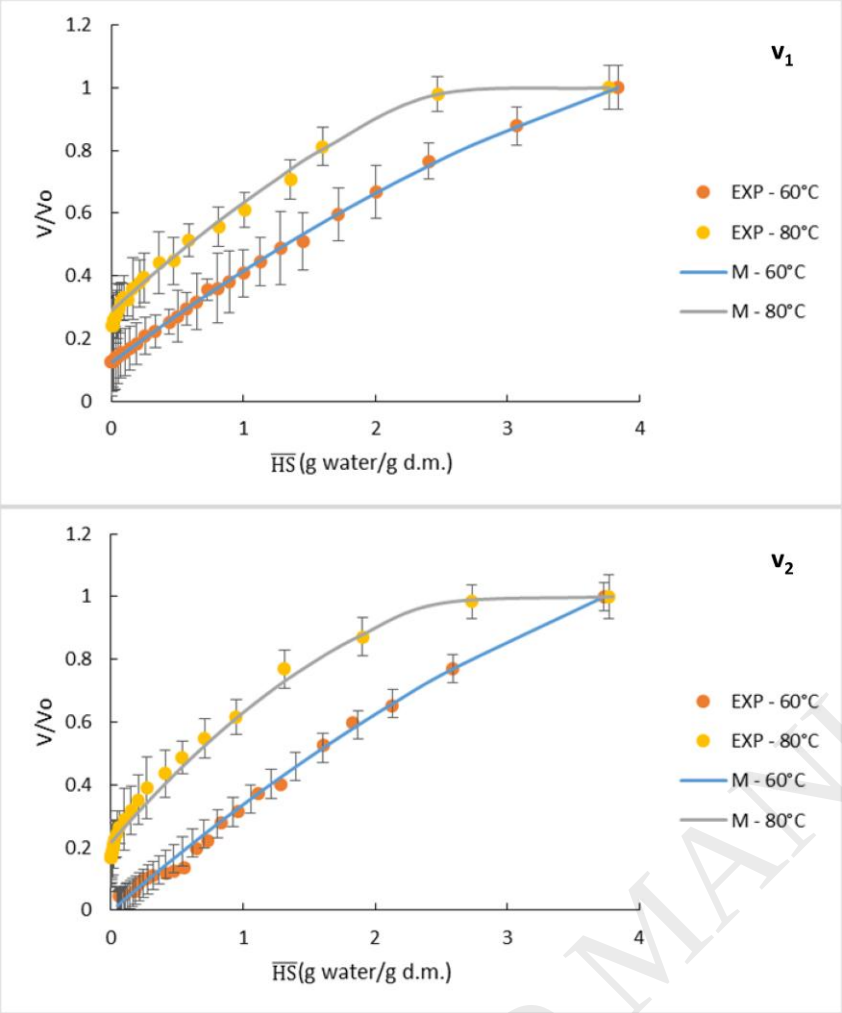

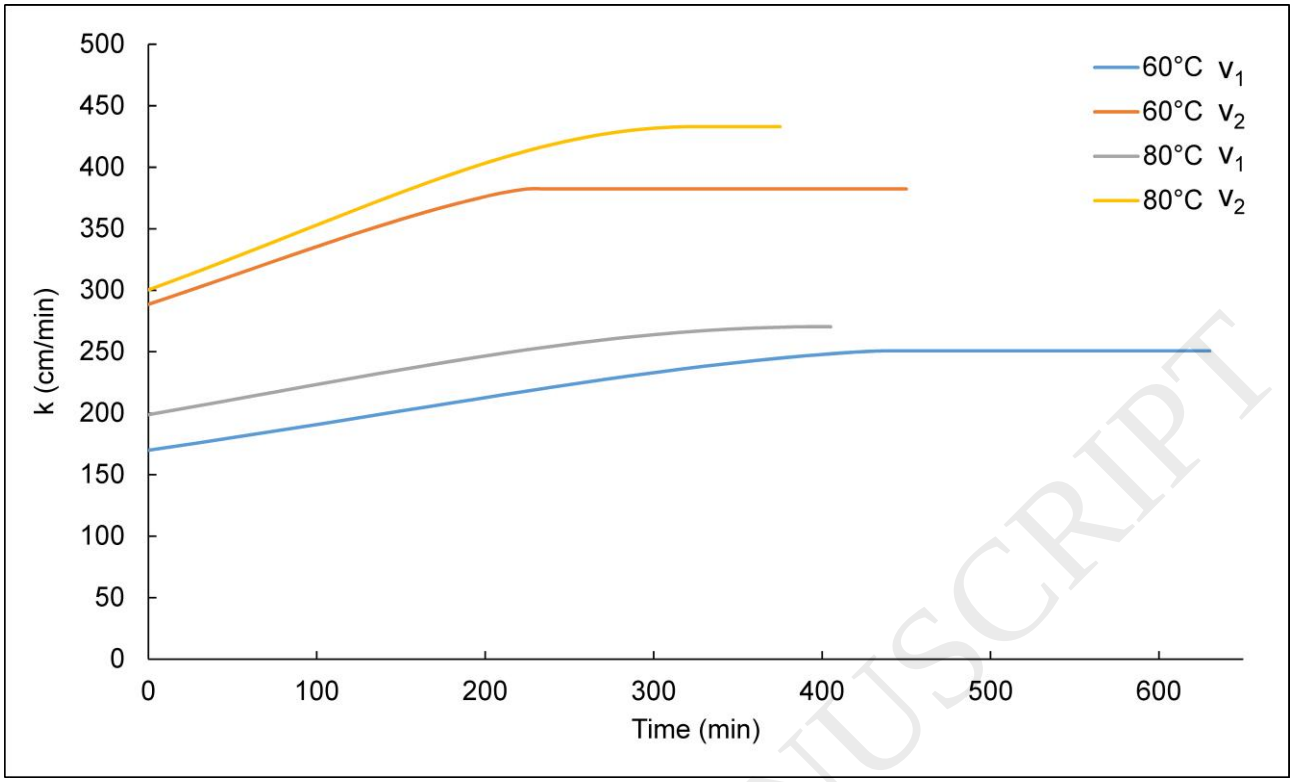

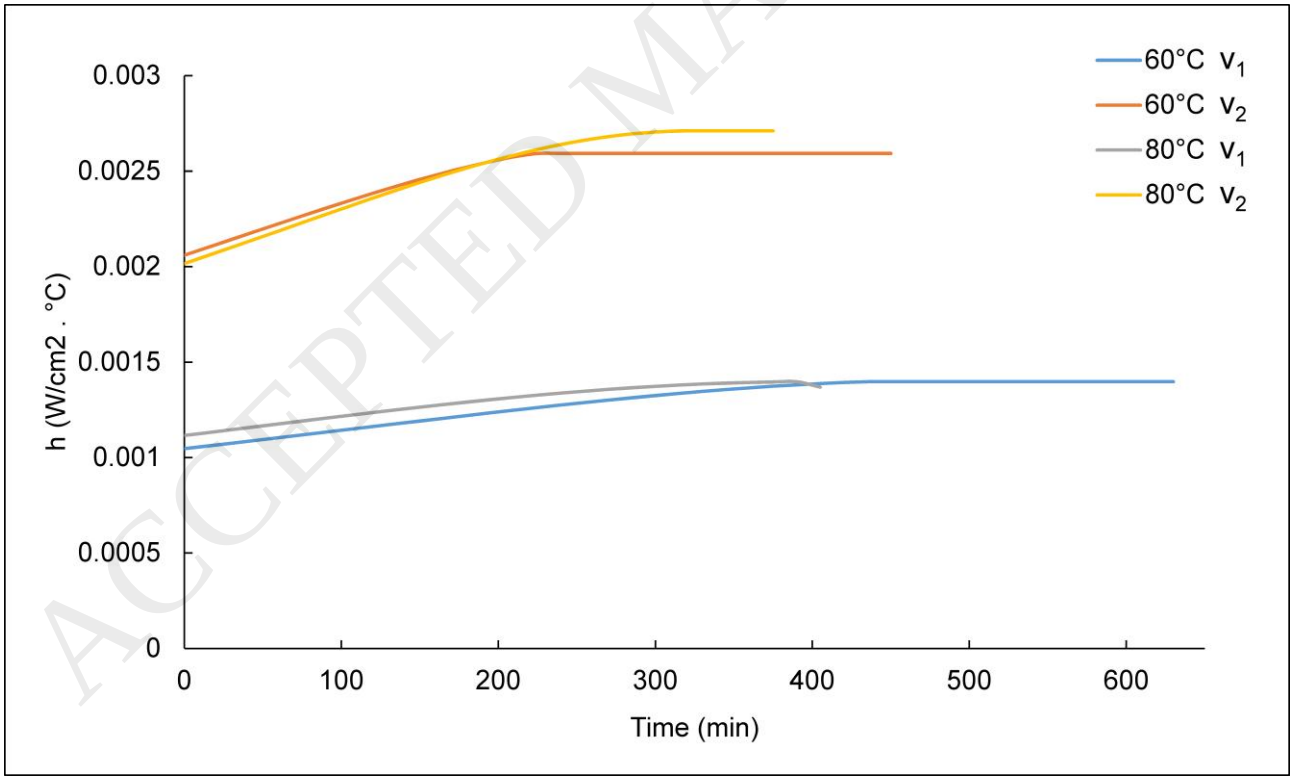

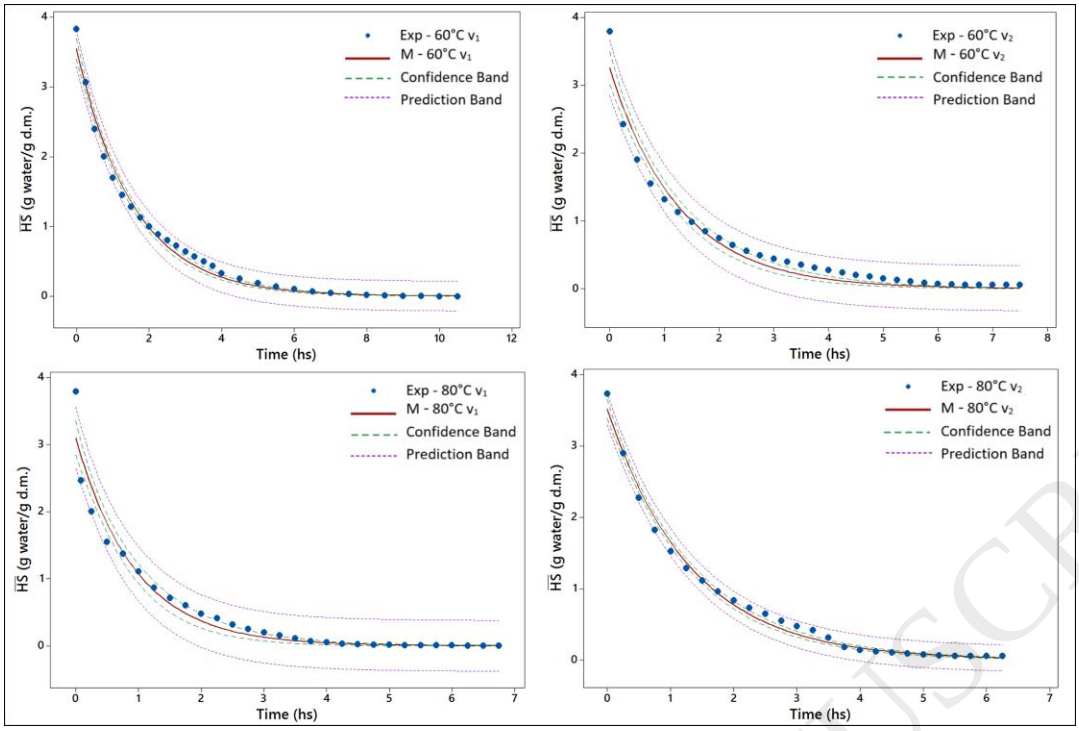

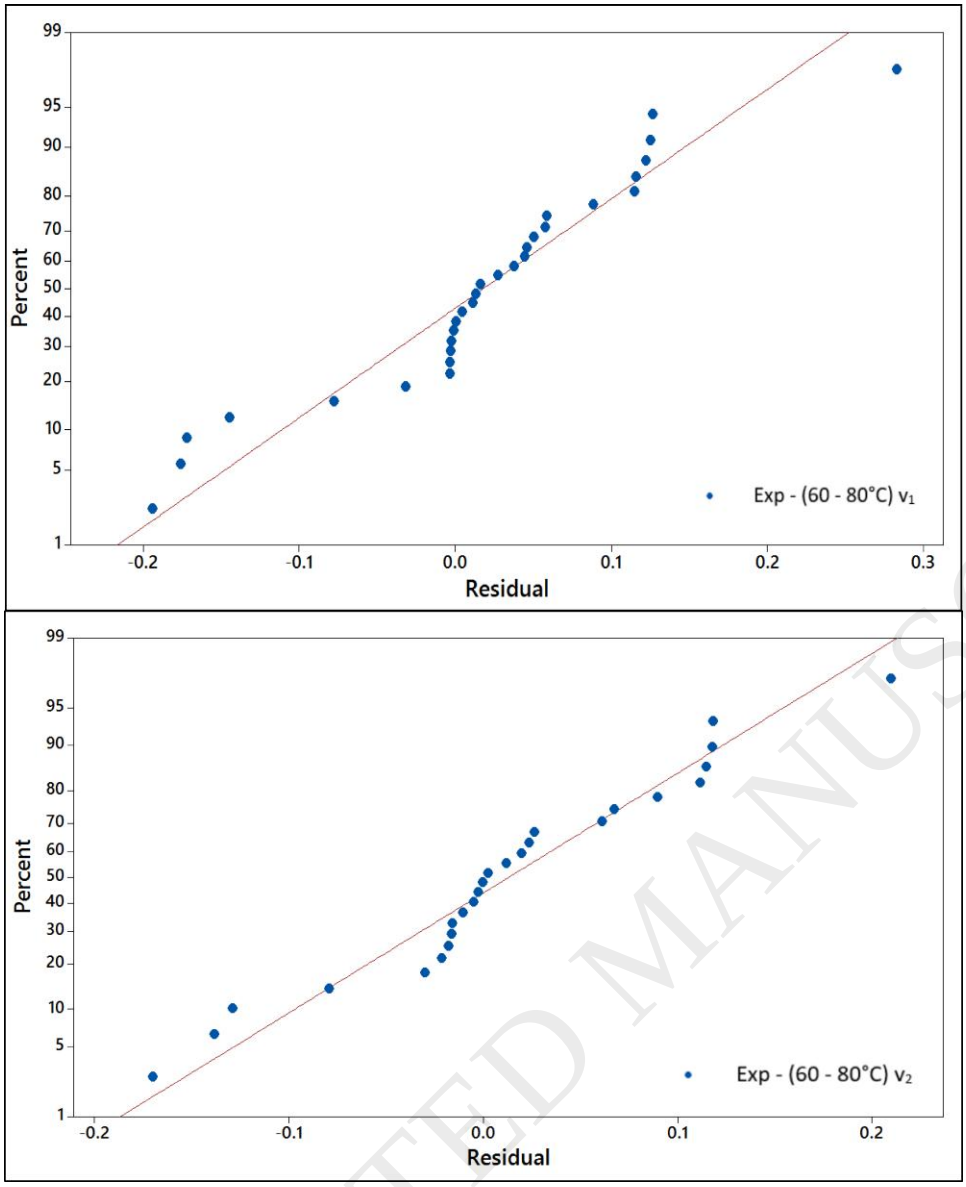

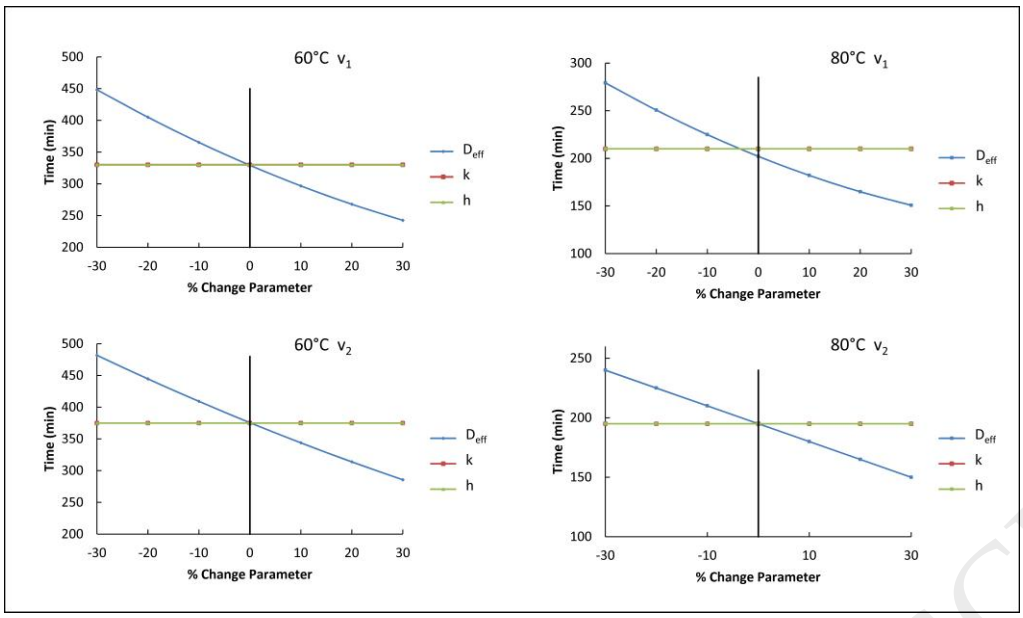

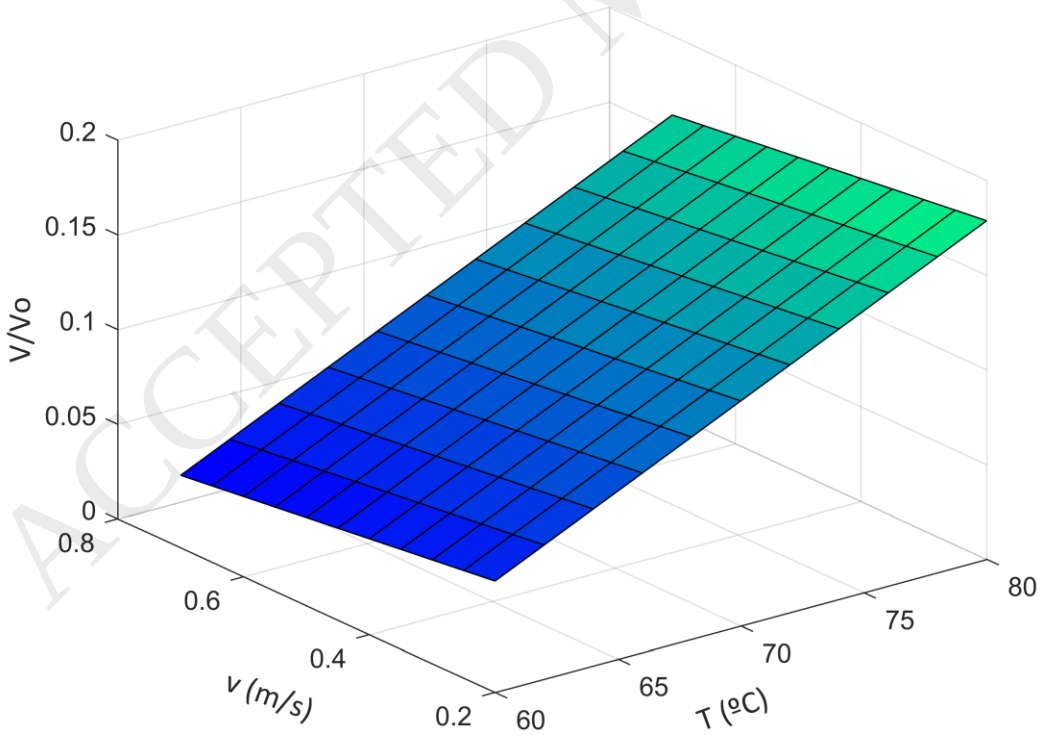

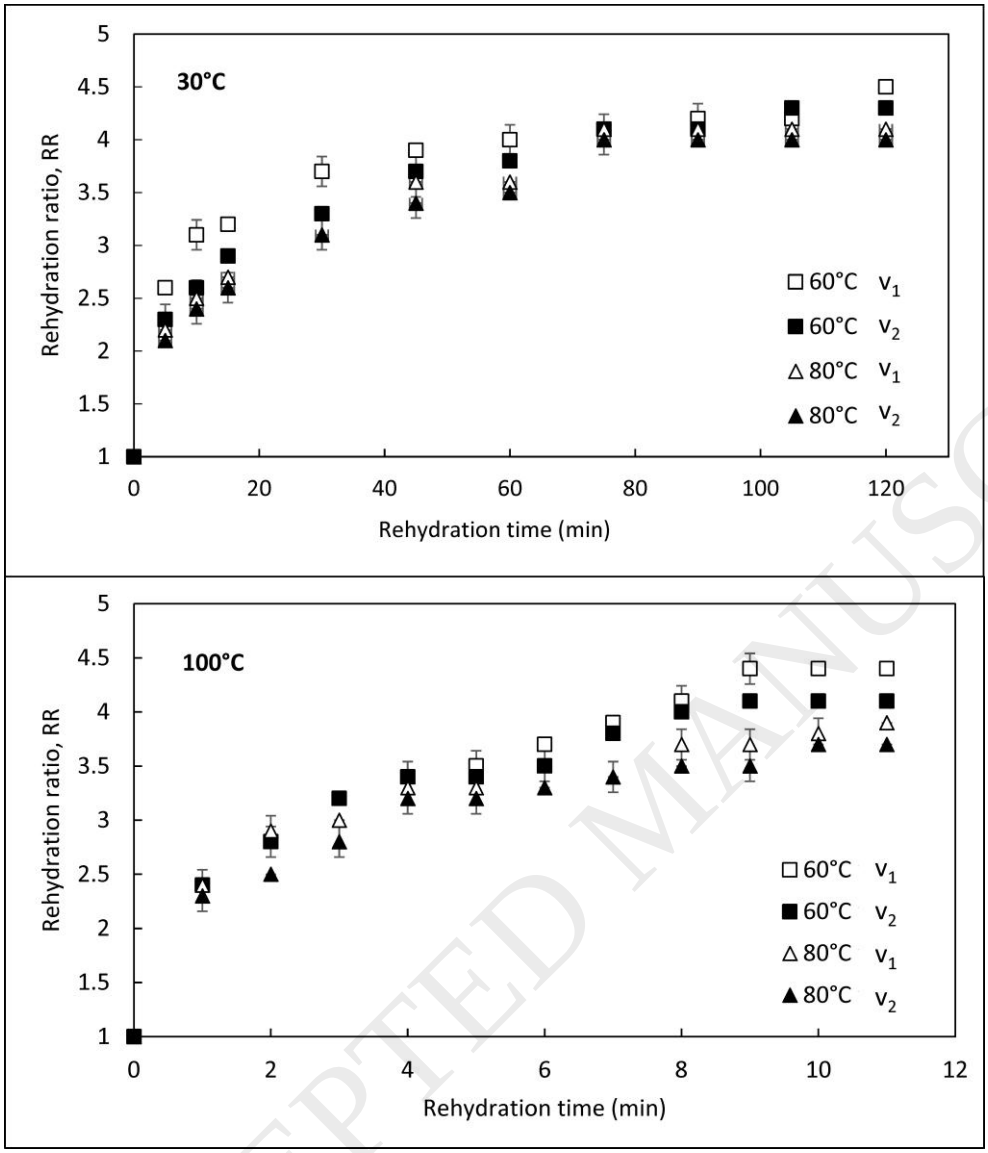

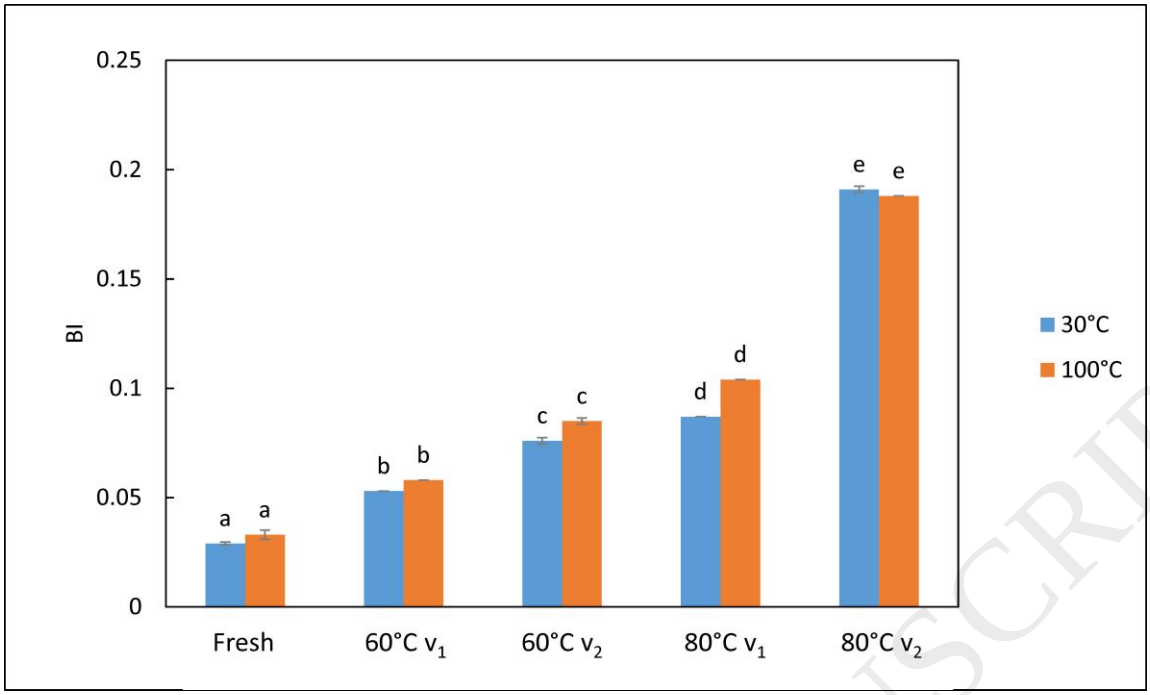

Table 1. Model input data

Shape variable or property	Value	Source
HS_o (g water. g dry matter^{-1})	3.970000	Experimental result
L_o (Lx_o, Ly_o, Lz_o) (cm)	0.500000	Experimental result
Cp_a (60°C) (J g^{-1} ºC^{-1})	1.008100	Geankoplis (1998)
Cp_a (80°C) (J g^{-1} ºC^{-1})	1.009000	Geankoplis (1998)
K_a (60°C) (W m^{-1} ºC^{-1})	0.000287	Geankoplis (1998)
K_a (80°C) (W m-1 ºC-1)	0.000302	Geankoplis (1998)
D_w (60°C) (cm^2 . s^{-1})	0.309000	Pakowski et al. (1991)
D_w (80°C) (cm^2 . s^{-1})	0.343000	Pakowski et al. (1991)
R (J . °C^{-1} mol^{-1})	0.831500	Geankoplis (1998)
P_a (Pa)	101325	Geankoplis (1998)

Table 2. Parameters of the second-order polynomial regression for Equation (8)

T_a (°C)	v (m/s)	d	e	f	R^2
60	0.2	-0.077	0.617	0.123	0.987
	0.7	-0.027	0.381	0.003	0.988
80	0.2	-0.040	0.624	0.274	0.989
	0.7	-0.070	0.490	0.242	0.981

Table 3. Adjustment data

T_a (°C)	v (m/s)	MSE Estimation of the diffusivity parameters (Eq. 9)	Estimation of the contraction parameters (Eq. 28)
60	0.2	0.085	0.064
	0.7	0.078	0.012
80	0.2	0.031	0.021
	0.7	0.022	0.021

Table 4. Final drying times at different conditions and adjustment data

T_a (°C)	v (m/s)	Drying time (min)	HS_{eq} (g water. g d.m.$^{-1}$)	R^2
60	0.2	630	0.001341 ± 0.000686	0.997
	0.7	450	0.001910 ± 0.015717	0.999
80	0.2	405	0.002213 ± 0.001312	0.999
	0.7	375	0.000855 ± 0.000605	0.999

Table 5. Parameters of the second-order polynomial regression for Equation (28)

T_a (°C)	v (m/s)	a	b	c	R^2
60	0.2	-0.077	0.617	0.123	0.986
	0.7	-0.027	0.381	0.003	0.987
80	0.2	-0.040	0.624	0.274	0.989
	0.7	-0.070	0.490	0.242	0.981

Table 6. ANOVA results

Response variable	Source	Sum of square	Degree of freedom	Mean of square	F-value	P-value	Significant
V/V0	Model	0.029	2	0.014	8.05	0.020	*
	Constant	0.156	2	0.014	10.94	0.000	**
	T_a	0.026	1	0.026	14.42	0.009	**
	v	0.003	1	0.003	1.68	0.243	
	Pure error	0.011	6	0.001			
	Total	0.040	8				

* Significant ($p < 0.05$).
** Extremely significant ($p < 0.01$)